Hadron Spectroscopy at CLAS and the Evolution of Strong Degrees of Freedom

R.W. Gothe[a]

[a]University of South Carolina,
Department of Physics and Astronomy, Columbia, SC 29208, USA

Understanding the strong force constitutes one of the biggest challenges in fundamental science that we can and have to tackle now as the needed experimental and theoretical tools become available. Perturbative Quantum ChromoDynamics (pQCD) at small distances, which is governed by quark and gluon fields, and Chiral Perturbation Theory (ChPT) at larger distances, which is governed by pion fields, are both already experimentally validated. However, strong fields at intermediate distances, where they generate about 98% of the total mass of nucleons and therefore of all normal matter, are not understood on similarly firm grounds. Electron scattering in particular serves as an ideal tool to investigate this intermediate region by measuring the resonance transition form factors of three-quark systems with varying momentum transfer and spatial resolution of the probe.

The status of the research program at Jefferson Lab to study baryon transition form factors and the evolution of the underlying effective degrees of freedom, or the origin of mass, will be exemplified by recent results in single and double-pion production obtained with CLAS by the Hall B collaborations. These results demonstrate that the separation of resonance and background contributions and therefore the extraction of the electro-coupling amplitudes of resonances become easier and cleaner at higher four-momentum transfers (Q^2). Furthermore, the double-pion in comparison to the single-pion channel shows a higher sensitivity to energetically higher lying resonances and a distinctly different dependence on the contributing background amplitudes. The combined analysis of the single- and double-pion data thus reduces model dependent uncertainties significantly, which allows us to extract the resonant electro-coupling amplitudes in an unprecedented quality.

1. INTRODUCTION

From the beginning, nucleons and baryons in general, have played an important role in the development of the quark model and of QCD. The concept of quarks itself was manifested by the study of baryon resonances. For many years the properties of the ground state and the excited states of baryons had been treated in terms of isobars or constituent quarks. However, currently we are at the threshold of measuring, describing, and comprehending these states in terms of effective QCD degrees of freedom and their evolution from ChPT to pQCD. The special importance of baryons is emphasized by recent QCD calculations on the lattice [1] that show evidence for a "Y-shape" color flux, indicating a genuine three-body force for baryons with stationary quarks and not a dominant two-body force that would generate "Δ-shape" color flux. This three-body force is an essential QCD feature that can be best studied in the three-quark baryon system. Laboratories worldwide are providing, and particularly their anticipated upgrades will soon provide, complementary hadronic or electromagnetic probes in the best suited energy range to perform precision experiments that test the nature of the strong force in this intermediate confinement regime. One of the leading laboratories in this research field is Jefferson Lab (JLab), where some of the most pressing experiments are planned and carried out. Examples reported here, will focus on the advantages of electro-excitations in exclusive single- and double-pion production channels and on baryon transition form factor measurements at low Q^2, to investigate the pion fields bridging the gap to ChPT, and at intermediate to high Q^2, to investigate the transition to the partonic degrees of freedom of the strong interaction.

2. EXCLUSIVE SINGLE-PION ELECTRO-PRODUCTION

A large portion of the nuclear physics community enthusiastically started to investigate baryon resonances as new optimized detector systems with large solid angle and momentum coverage like CLAS and new high-intensity continuous electron beams like at JLab became available. The high versatility of the provided electromagnetic probes that have negligible initial state interaction have produced intriguing results ever since. It was realized that the isoscalar or isovector, and the electric, magnetic or longitudinal nature of the coupling to hadronic matter, probes different aspects of the strong interaction. However, the desired versatility of the electromagnetic probe comes with the complication that it mixes all the different coupling amplitudes simultaneously into the measured cross sections. The ability to resolve the interfering amplitudes has already been demonstrated in the case of the N to $\Delta(1232)$ transition, where the small resonant scalar quadrupole (R_{SM}) amplitude could be extracted with respect to the dominant magnetic dipole amplitude with absolute systematic uncertainties of typically 0.5% [2,4,5,9] at intermediate momentum transfers of $0.2\,(GeV/c)^2 < Q^2 < 1.0\,(GeV/c)^2$, see Figures 1 and 2. To obtain such precision results for the extraction of isolated resonance parameters, additional isospin channels and polarization observables had been measured to disentangle the individual resonant and non-resonant coupling amplitudes [10–12]. The same precision of 0.5% was achieved for $R_{EM} = -2.5\%$ [13] in photo-production for an even more complete set of observables, see Figure 1, and the fundamental approach of how to perform a complete experiments in pseudo-scalar photo-production is described in [14].

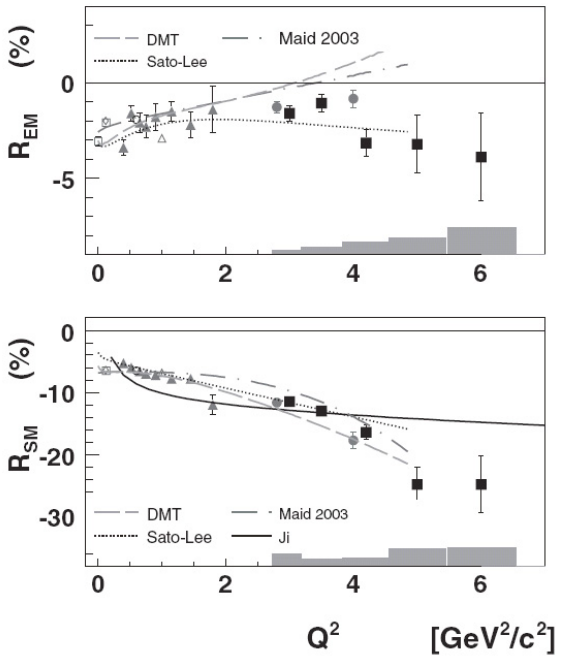

Figure 1. The N to $\Delta(1232)$ transition form factor ratios R_{EM} (upper panel) and R_{SM} (lower panel) [2]. The experimental results are from JLab, MAMI, ELSA, and Bates [3–8,11].

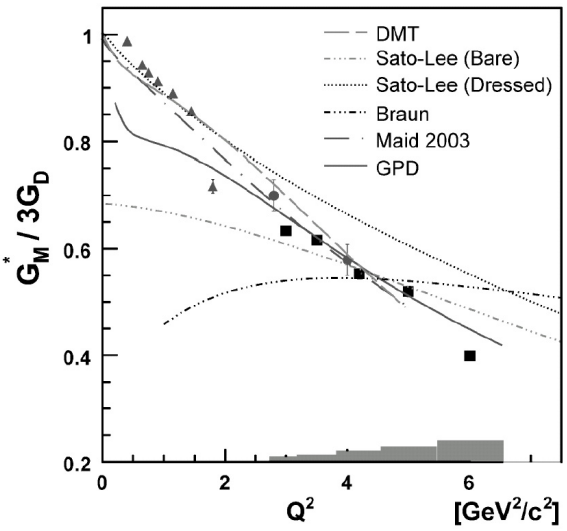

Figure 2. The magnetic N to $\Delta(1232)$ transition form factor normalized to the dipole form factor $G_M^*/3G_D$ [2]. The experimental results are from JLab [3,4,6].

Preliminary JLab [15] results at low four momentum transfers down to $0.1\,(GeV/c)^2$ follow the known constant behavior of R_{EM} and the constantly decreasing behavior of R_{SM} for increasing Q^2. The extrapolation of both ratios to even smaller Q^2 values seems to agree with the real photon point R_{EM} results [8,16] or with Siegert limit respectively, whereas the R_{SM} dis-

agrees with the MAMI [17] and Bates [18] results at $Q^2 = 0.127\,(GeV/c)^2$. A further extension into the momentum transfer region of $0.01\,(GeV/c)^2 < Q^2 < 0.1\,(GeV/c)^2$, where little to no results are available, is experimentally challenging. How strongly this lack of data impacts the comprehension of the strong interaction in this regime is illustrated in Figure 3. Intuitively

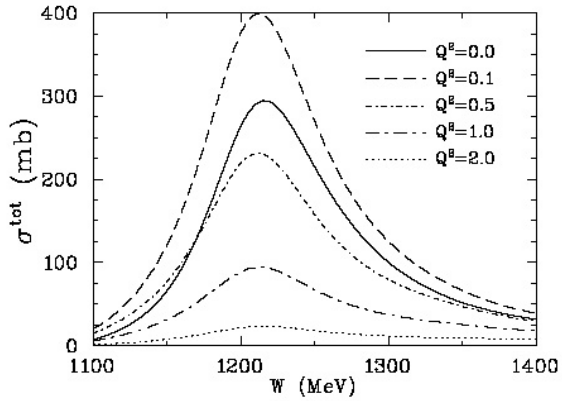

Figure 3. Total cross section of the $p\pi^0$ electroproduction for different four momentum transfers in $(GeV/c)^2$ [19].

one would expect that the total cross section is largest at $Q^2 = 0\,(GeV/c)^2$, since the N to $\Delta(1232)$ transition factors should drop with increasing Q^2. However, the total cross section at $Q^2 = 0.1\,(GeV/c)^2$ is significantly larger than at the real photon point, $Q^2 = 0\,(GeV/c)^2$ [19]. This can only be explained by a strong longitudinal coupling of the virtual photon to the nucleon and by the fact that the kinematical suppression of the longitudinal coupling drops for $Q^2 \to 0\,(GeV/c)^2$ much faster than the transition form factors for increasing Q^2.

On the other side pQCD predicts in the high Q^2-limit, by neglecting higher twist contributions, a $1/Q^4$ fall-off of G_M^*, a R_{EM} of $+1$, and a Q^2 independent R_{SM}. The experimental results, which are now available up to $6\,(GeV/c)^2$ as shown in Figures 1 and 2, reveal no indication of the predicted behavior in any of the three cases, but rather follow the same overall trend of the established results in the lower Q^2 region. This is particularly striking in the case of the magnetic N to $\Delta(1232)$ transition form factor G_M^*, where simple constituent counting rules would demand the $1/Q^4$ dipole form; as well as in the case of the R_{EM}, that is defined by the helicity conserving amplitude $A_{\frac{1}{2}}$ and the helicity non-conserving amplitude $A_{\frac{3}{2}}$, where the simple argument of helicity conservation at high momentum transfers demands $A_{\frac{3}{2}} \ll A_{\frac{1}{2}}$, which directly leads to the prediction that $R_{EM} \to +1$. Thus the obvious question is, at which Q^2 should helicity conservation as well as a pQCD based description start to dominate. Perhaps momentum transfers of up to $6\,(GeV/c)^2$ are still not high enough.

We may attempt to deduce the answer from the lattice calculation (LQCD) [20] of the quark mass M as function of the quark propagator momentum q and the fact that helicity is conserved when the momentum of the hadron is large compared to its mass $q \gg M$. In contrast to the momentum transfer, that has to be shared between all three quarks in exclusive reactions, the angular momentum transfer in resonance excitations can either involve several quarks and more complicated configurations or in principle also only one quark. The quark mass function in Figure 4 gives at $q = 2\,GeV/c$ a quark mass of the order of

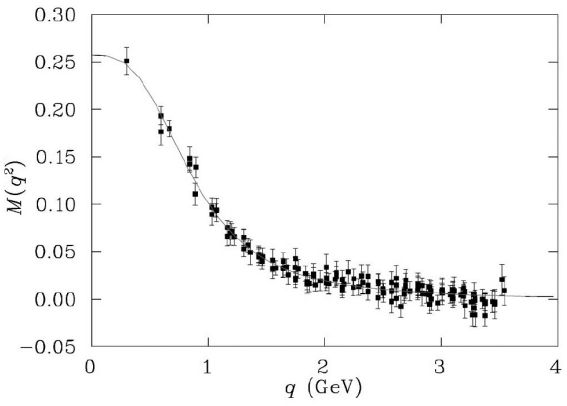

Figure 4. Lattice QCD calculation [20] of the quark mass in the chiral limit, where q is the momentum variable of the tree-level quark propagator using the Asquat action. Similar results have been obtained in the Dyson-Schwinger approach [21,22] and the instanton framework [23].

$15\,MeV/c^2$, which roughly corresponds to a momentum transfer of $Q^2 = 4\,(GeV/c)^2$ for the simplest assumption that only a single quark absorbs the angular momentum introduced by the virtual photon. Here the condition for helicity conservation would definitely be fulfilled, but it would break down for $q \leq 1\,GeV/c$, where quark mass steeply increases with decreasing quark momentum. These arguments lead to the prediction that for resonances that conserve angular momentum on the single quark level, the helicity conserving amplitude $A_{\frac{1}{2}}$ should dominate the helicity non-conserving amplitude $A_{\frac{3}{2}}$ at $Q^2 \geq 1\,(GeV/c)^2$. This predicted behavior is indeed clearly visible for the preliminary $D_{13}(1520)$ helicity amplitudes $A_{\frac{1}{2}}$ and $A_{\frac{3}{2}}$ and the corresponding helicity asymmetry [24]. It is therefore not only important to extend the transition form factor measurements for the N to $\Delta(1232)$ excitation to even higher momentum transfers, but also to investigate the Q^2 evolution of exclusive transition form factors to as many higher lying resonances as possible. In the first case we need to push the measurements of exclusive observables and their theoretical description towards the onset of partonic degrees of freedom. These experiments require the JLab and CLAS upgrades to $12\,GeV$. In the latter case preliminary results of the Q^2 dependencies of the helicity coupling amplitudes for the higher lying resonances P_{11}, D_{13}, S_{11}, and F_{15} have already been extracted up to $4\,(GeV/c)^2$ [24]. Since especially the Roper (1440) resonance parameters have always been notoriously hard to extract, the variety of different theoretical approaches to describe them is extensive and includes q^3, $q^3 + q\bar{q}$ cloud, and $q^3 + g$ hybrid quark models as well as dynamical coupled channel and $N + \sigma$ molecule models. Figure 5 illustrates the quality of the results and both the shortcomings or strengths of various model predictions. The low Q^2 behavior is best described by meson cloud models like [36], while the high Q^2 behavior is described more consistently by the relativistic light-front quark models like [31,32,35]. Still maybe the most interesting new result is that here, as well as in the double-pion production channel, many resonances are easier to isolate at higher Q^2 than at

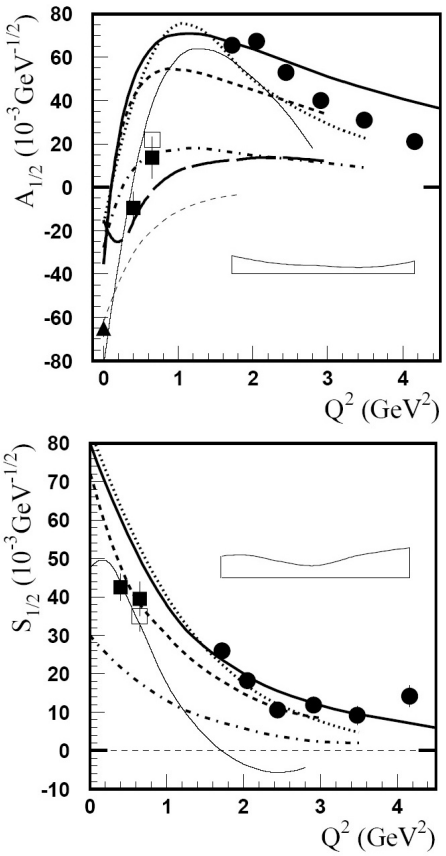

Figure 5. Full circles are the most recent helicity amplitudes for the N to Roper(1440) transition [25] based on CLAS π^+ electro-production data [26]. The bands represent the systematic uncertainties. The full boxes are the results obtained from CLAS data [27,28], and the open boxes represent the results of the combined analysis of CLAS single π and 2π electro-production data [29]. The full triangle at $Q^2 = 0\,(GeV/c)^2$ is the RPP estimate [30]. The bold curves correspond to relativistic light-front quark models: dotted, dashed, dash-dotted, long-dashed, and solid curves are from [31–35], respectively. The thin solid curves are calculations obtained for a quark core dressed by a meson cloud [36], and the thin dashed curves for a $q^3 + g$ hybrid state [37].

or close to the real photon point. The preliminary results of the extracted resonant multipole amplitudes M_{1-} and E_{0+} of the Roper (1440) and the $S_{11}(1535)$ respectively, demonstrate how dra-

matically the resonance behavior of the real and the imaginary part of these two resonant amplitudes are enhanced at higher Q^2 compared to the real photon point [24]; where the extracted resonant multipole amplitudes reflect the difficulties of isolating the Roper resonance, which even does not produce a peak in the inclusive cross section, and the $S_{11}(1535)$, which typically had to be investigated in the η production channel to allow a cleaner separation from neighboring resonances and background contributions.

3. EXCLUSIVE DOUBLE-PION ELECTRO-PRODUCTION

The studies of double-pion production by real and virtual photons [38–50] clearly show the capability of this exclusive channel to provide important information on N^* electro-coupling amplitudes and hadronic decay parameters for most of the excited nucleon states. The information on N^* parameters extracted from double-pion electro-production is complementary to that obtained in the single-pion channel. The single-pion channel is mostly sensitive to nucleon resonances in the invariant mass W range below $1.7\,GeV$ [51], while the double-pion channel exhibits contributions from both low lying $W \leq 1.6\,GeV$ and high lying $1.6\,GeV \leq W \leq 3.0\,GeV$ resonance states. According to the scattering data from experiments with hadronic probes [30] as well as quark model expectations [52], most of the high lying excited states should decay substantially or even dominantly into either $\Delta\pi$ or $N\rho$ intermediate states and thus into two pions. This makes the electromagnetic exclusive double-pion production an important tool in the investigation of nucleon resonances and reaction dynamics as well as in the search for missing baryon states, where the term missing resonances refers to the fact that quark models based on the flavor blindness of the strong interaction predict more nucleon excitations than found experimentally. An additional advantage of the double-pion production channel is the genuinely different non-resonant contributions, which underlines again the complementarity to the single-pion analysis. Thus, the double-pion channel is a promising way to obtain comprehensive data on the Q^2 evolution of electromagnetic form factors for most of the baryonic states. Preliminary double-pion results [53,54] from simultaneous fits to nine single-differential cross section projections, based on a phenomenological isobar model approach, are available for $P_{11}(1440)$, $D_{13}(1520)$, $S_{31}(1650)$, $S_{11}(1650)$, $F_{15}(1685)$, $D_{13}(1700)$, $D_{33}(1700)$, $P_{13}(1720)$, $F_{35}(1905)$, $P_{33}(1920)$, and $F_{37}(1950)$ as well as the indication for a new $3/2 + (1720)$ resonance that couples significantly weaker to $N\rho$ and stronger to $\Delta\pi$ than the $P_{13}(1720)$ [30].

4. COMBINED ANALYSIS

An effective way to insure a credible separation between resonant and non-resonant mechanisms may indeed be the combined analysis of the single- and double-pion channel, which accounts for the major part of the total virtual photon cross-section in the N^* excitation region. Since both channels have entirely different non-resonant contributions, a successful combined description of all observables measured in the single- and double-pion electro-production off nucleons with a common set of N^* electro-coupling amplitudes and hadronic parameters would ensure a reliable separation between the resonant and non-resonant contributions in both exclusive channels. Such a successful description of all observables in both channels with a common set of N^* electro-coupling and hadronic parameters has already been achieved in a combined analysis of CLAS data at $Q^2 = 0.65\,(GeV/c)^2$ [29] (see also Fig. 5), providing strong support for the phenomenological approaches [53,55] used in the CLAS data analysis.

REFERENCES

1. H. Ichie, V. Bornyakov, T. Steuer, and G. Schierholz, hep-lat/0212024 (2002).
2. M. Ungaro et al., Phys. Rev. Lett. 97, 112003 (2006).
3. I. G. Aznauryan, Phys. Rev. C 67, 015209 (2003).
4. K. Joo et al., Phys. Rev. Lett. 88, 122001 (2002).

5. R.W. Gothe, Proceedings of NSTAR 2002, World Scientific (2003).
6. V.V. Frolov et al., Phys. Rev. Lett. 82, 45 (1999).
7. C. Mertz et al., Phys. Rev. Lett. 86, 2963 (2001).
8. R. Beck et al., Phys. Rev. C 61, 035204 (2000).
9. G. Laveissiere et al., Phys. Rev. C 69, 045203 (2004).
10. K. Joo et al., Phys. Rev. C 70, 042201 (2004).
11. J.J. Kelly et al., Phys. Rev. Lett. 95, 102001 (2005).
12. H. Egiyan et al., Phys. Rev. C 73, 025204 (2006).
13. R.A. Arndt et al., nucl-th/9708006 (1997) and Phys. Rev. C 66, 055213 (2002).
14. I.S. Barker, A. Donnachie, and J.K. Storrow, Nucl. Phys. B 95 (1975).
15. Preliminary JLab Results, L.C. Smith, Private Communication (2007).
16. G. Blanpied et al., Phys. Rev. Lett. 79 (1997).
17. T. Pospischil et al., Phys. Rev. Lett. 86 (2001).
18. N.F. Spaveris et al., Phys. Rev. Lett. 94, 022003 (2005).
19. R. Arndt et al., arXiv:nucl-th/0301068 or Proceedings of NSTAR2002, World Scientific (2003).
20. P.O. Bowman et al., Phys. Lett. D 66, 014505 (2002) and arXiv:hep-lat/0209129 (2002).
21. M.S. Bhagwat et al. arXiv:nucl-th/0304003 (2003).
22. H. Iida et al., Nucl. Phys. Proc. Suppl. 141 (2005).
23. D. Diakonov and V. Petrov, Phys. Lett. B 147 (1984).
24. Preliminary JLab Results, K. Park and I. Aznauryan, Private Communication (2008).
25. I. Aznauryan et al., arXiv:nucl-ex/0804.0447 (2008).
26. K. Park et al., Phys. Rev. C 77, 015208 (2008).
27. I.G. Aznauryan et al., Phys. Rev. C 71, 015201 (2005).
28. K. Joo et al., Phys. Rev. Lett. 88, 122001 (2002); K. Joo et al., Phys. Rev. C 68, 032201 (2003); K. Joo et al., Phys. Rev. C 70, 042201 (2003); H. Egiyan et al., Phys. Rev. C 73, 025204 (2006).
29. I.G. Aznauryan et al., Phys. Rev. C 72, 045201 (2005).
30. S. Eidelman et al., Phys. Lett. B 592 (2004).
31. S. Capstick and B.D. Keister, Phys. Rev. D 51 (1995).
32. H.J. Weber, Phys. Rev. C 41, 2783 (1990).
33. F. Cardelli et al., Phys. Lett. B 397 (1997).
34. B. Julia-Diaz, Phys. Rev. C 69, 035212 (2004).
35. I.G. Aznauryan et al., Phys. Rev. C 76, 025212 (2007).
36. F. Cano and P. Gonzalez, Phys. Lett. B 431 (1998).
37. Z. Li and V. Burkert, Phys. Rev. D 46 (1992).
38. M. Ripani et al., Phys. Rev. Lett. 91, 022002 (2003).
39. M. Bellis et al., Proceedings of NSTAR2004, World Scientific (2004).
40. M. Battaglieri et al., Phys. Rev. Lett. 87, 172002 (2001).
41. S. Strauch et al., Phys. Rev. Lett. 95, 162003 (2005).
42. G. Fedotov et al., CLAS Analysis Note, June 2006.
43. U. Thoma, Int. J. Mod. Phys. A 20 (2005).
44. C. Wu et al., Eur. Phys. J A 23 (2005).
45. Y. Assafiri et al., Phys. Rev. Lett. 90, 222001 (2003).
46. J. Ahrens et al., Phys. Lett. B 624 (2005).
47. M. Kotulla et al., Phys. Lett. B 578 (2004).
48. W. Langgartner et al., Phys. Rev. Lett. 87, 052001 (2001).
49. F. Harter et al., Phys. Lett. B 401 (1997).
50. A. Braghieri et al., Phys. Lett. B 363 (1995).
51. V. Burkert and T.-S.H. Lee, Int. J. Mod. Phys. E 13 (2004) and nucl-ex/0407020.
52. S. Capstick and W. Roberts, Prog. Part. Nucl. Phys. 45 (2000).
53. V. Mokeev et al., arXiv:hep-ph/0512164; Phys. of Atom. Nucl. 66 (2003); Phys. of Atom. Nucl. 64 (2001).
54. Preliminary JLab Results, V. Mokeev, Private Communication (2008).
55. I.G. Aznauryan, Phys. Rev. C 68, 065204 (2003) and Phys. Rev. C 67, 015209 (2003).